Electronic Supplementary Material (ESI) for Journal of Materials Chemistry C.

Electrochemistry of new generation conformal polyaniline/carbon scaffolds with monodisperse nanopores and high capacitance

Chengying Ai,[†] Irina V. Chernyshova,[‡] Erin L. Gawron, [†] Sathish Ponnurangam, [†] and Viola I. Birss,[§]*

[†]Department of Chemical and Petroleum Engineering, Schulich School of Engineering, University of Calgary, Calgary, AB, Canada, T2N 1N4

[§]Department of Chemistry, University of Calgary, Calgary, AB, Canada, T2N 1N4

[‡]Department of Geoscience and Petroleum, Norwegian University of Science and Technology (NTNU), NO-7031 Trondheim, Norway.

*Corresponding author: birss@ucalgary.ca

Supplementary Information

Table S1. Characteristics of conformal PANI/carbon composites reported in the literature

PANI Coating Method	Carbon Substrate (pore sizes)	Coating Time (h)	PANI Layer Thickness (nm)	C_{sp} (F/g)		BET Surface Area (m^2/g)		Ref[Δ]
				Carbon	*PANI/ Carbon*	*Carbon*	*PANI/ Carbon*	
Cyclic Voltammetry	**NCS membrane** (50-85 nm pores; 11-13 nm pore neck)	0.3 - 1.3	3-15	18[*]	95 – 332[¶]	145[*]	138[‡]	**This work**
Chemical Polymerization	Carbon powder (20 µm, 2 µm and 10 – 100 nm pore dia)	0.5 - 10.5	2-50	60	150 – 239	-		**(26)**
Oxidative Chemical Vapor Deposition	Carbide- derived carbon powder (0.81, 1.7, and 3.4 nm pore dia)	NA	1-2 nm	60	155	530	470	**(27)**
Cyclic Voltammetry	3DOM carbon monolith (550 nm pore size; 100 nm pore neck)	2.2	-	140	248-352	1164	-	**(28)**

[*] Data for the NCS with a 85 nm pore size (NCS-85) are shown as an example.

[¶] These data were obtained using 3, 6 and 12 CV cycles (5 mV/s) of PANI deposition into the NCS-85 caffold, producing the PANI-3/NCS-85, PANI-6/NCS-85, and PANI-12/NCS-85 composites, respectively.

[‡] Data for PANI-6/NCS-85 are shown here as an example.

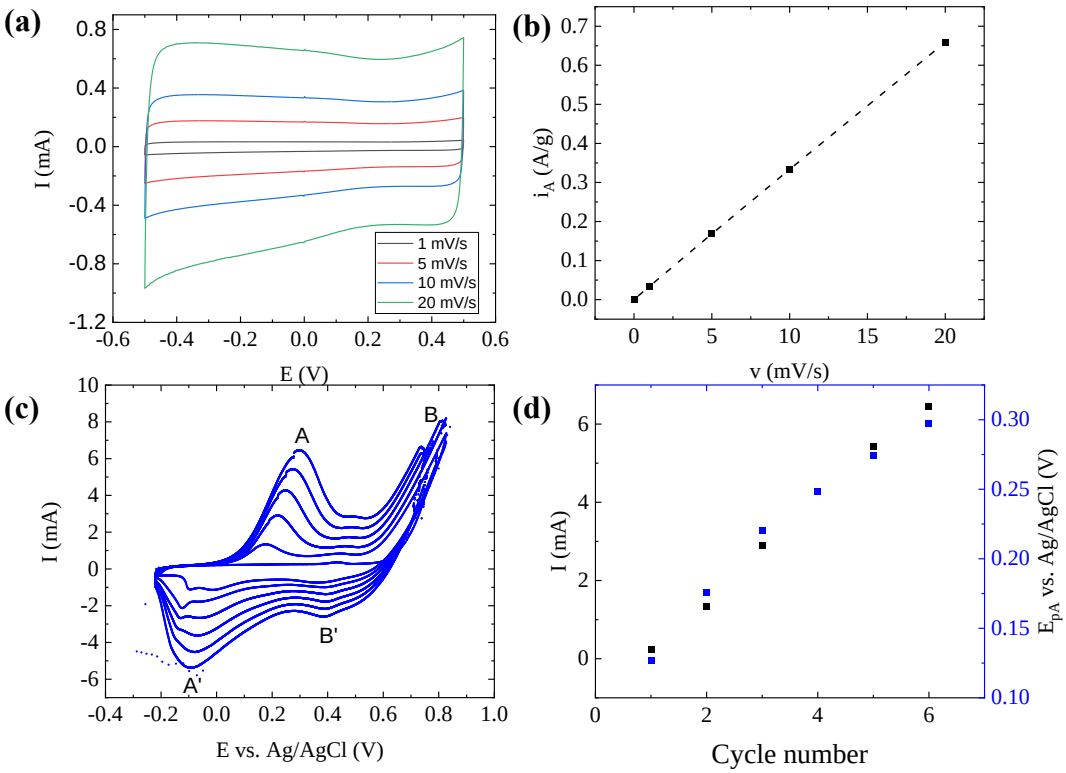

Figure S1. (a) Cyclic voltammograms of NCS-50 in N_2-saturated 3 M NaCl solution at various scan rates (1, 5, 10, and 20 mV/s). (b) shows the relationship between the anodic current density at 0 V and the scan rate for NCS-50. (c) Electrochemical polymerization of aniline at NCS-50 by scanning between -0.22 to +0.83 V vs. Ag/AgCl in 1 M H_2SO_4 + 0.1 M aniline. (d) Peak A current and potential (from (c)) vs scan rate.

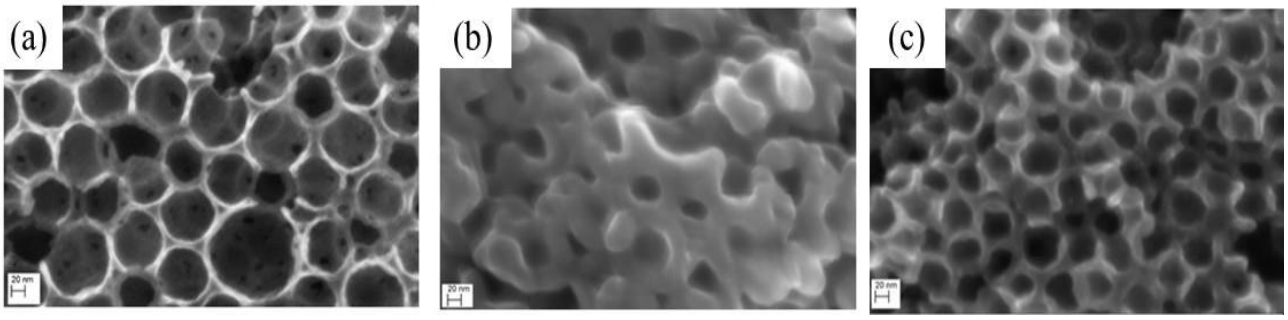

Figure S2. FESEM images of (a) PANI-3/NCS-85, (b) PANI-12/NCS-85 and (c) PANI-6/NCS-50.

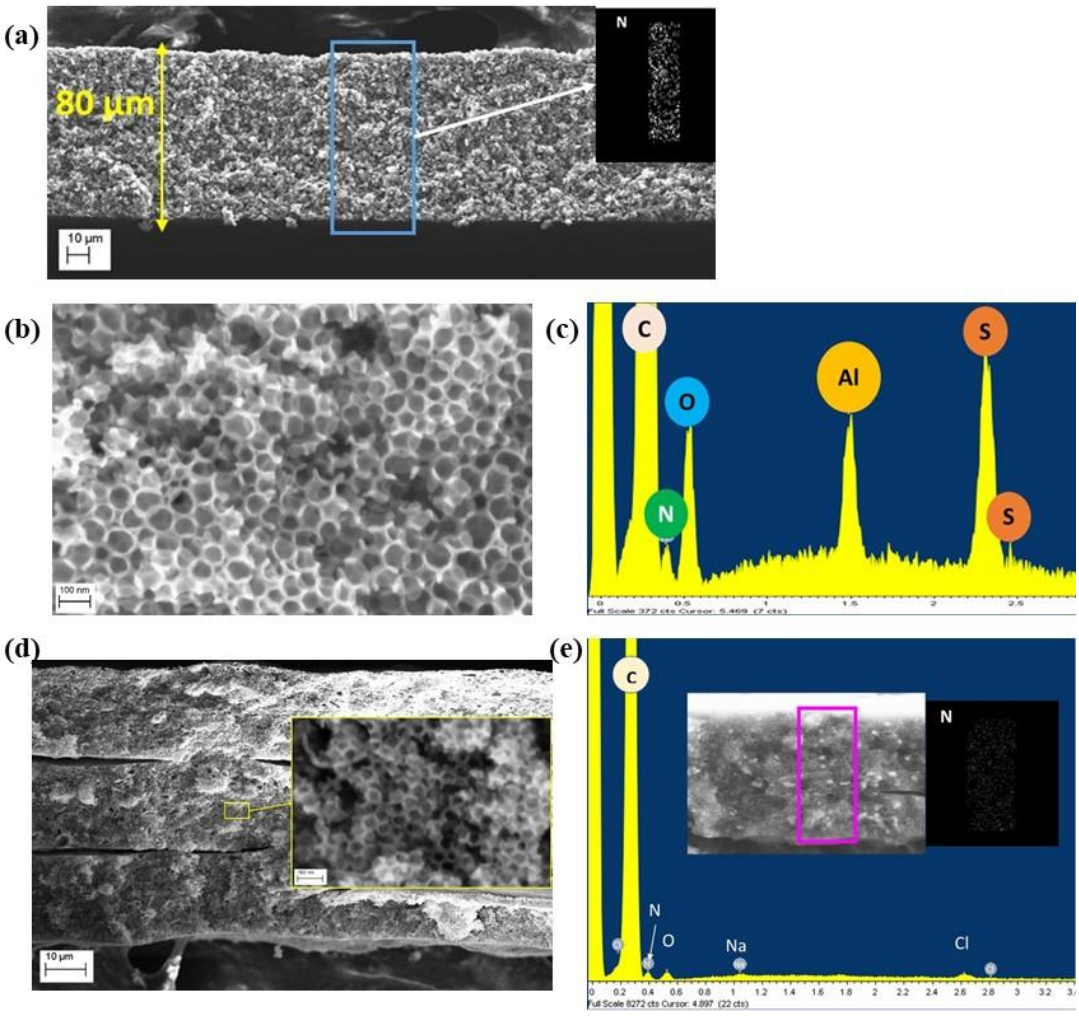

Figure S3. (a) Cross-sectional SEM image of PANI-6/NCS-85, where the thickness of the PANI-6/NCS-85 film is roughly 80 µm. The inset image shows an EDX map of the blue rectangular area in the cross-section in (a), showing a uniform distribution of nitrogen across the film. (b) Zoomed-in FESEM image in the middle of the cross-section of the PANI-6/NCS-85 film, while (c) shows the EDX spectrum of the blue rectangular area in the cross-sectional image in (a), verifying the presence of nitrogen throughout the PANI/NCS films. (d) FESEM of the cross-section of PANI-6/NCS-50. The image in the inset shows a higher magnification image of the middle of the cross-section of PANI-6/NCS-50. (e) EDX map of the cross-section of PANI-6/NCS-50, where N is again seen to be evenly distributed throughout the film.

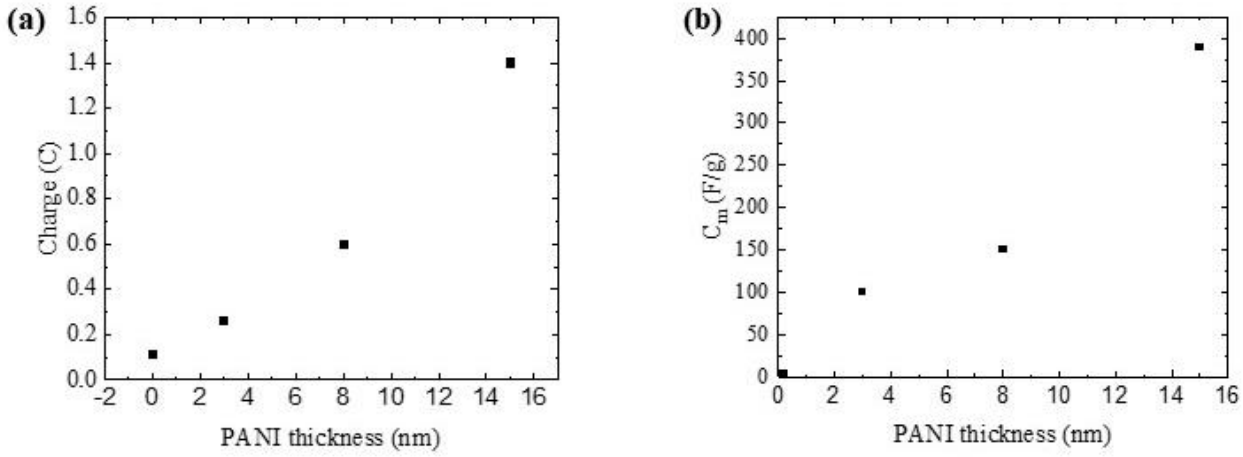

Figure S4. (a) Charge from PANI growth CVs (**Fig. 3a**) vs. PANI film thickness inside the PANI-3/NCS-85, PANI-6/NCS-85 and PANI-12/NCS-85 films, obtained from FESEM images (**Figs. 2c & S2**). (b) Gravimetric capacitance (C_m) of the PANI-X/NCS-85 composites vs. the PANI coating thickness.

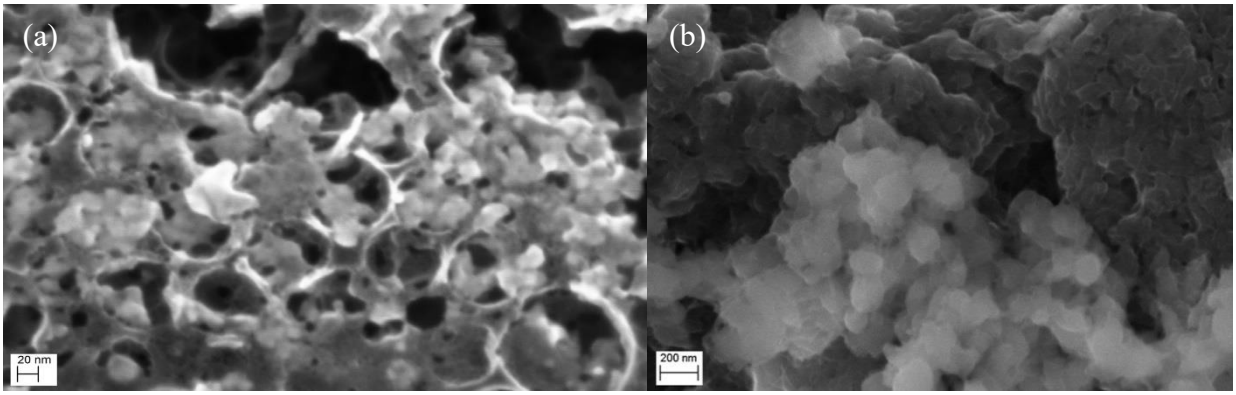

Figure S5. FESEM images of the PANI-coated NCS prepared by (a) scanning between -0.22 to 0.83 V at 50 mV/s for 60 cycles, and (b) scanning between -0.22 to 1.4 V at 5 mV/s for 1 cycle. These images show that (a) at high growth rates, the polymer forms clusters inside the pores on the NCS surface and (b) the polymer grows only at the outer surface when very positive upper limits are used during growth.

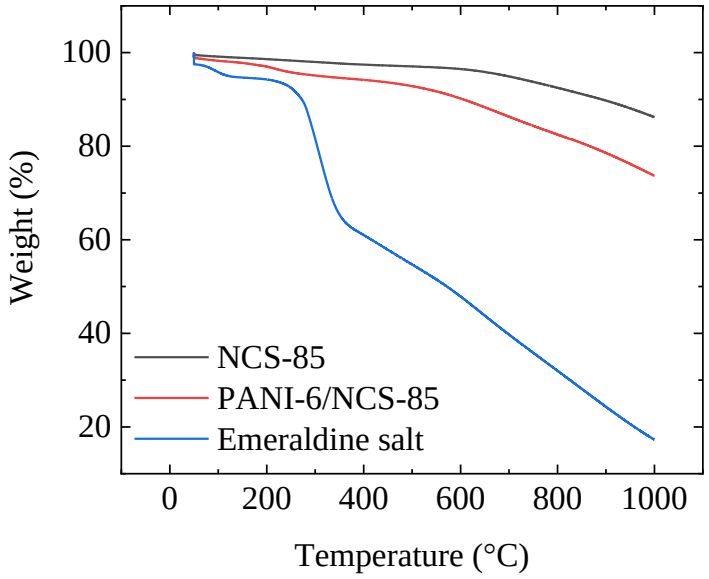

Figure S6. TGA of NCS-85, the PANI-6/NCS-85 composite and the commercial emeraldine salt (ES) while heating from 50 ˚C to 1000 ˚C in nitrogen at a ramp rate of 10 ˚C/min.

The thermogravimetric analyses were performed for commercial ES powder (grey), NCS-85, and a composite of PANI-6/NCS-85. The TGA data for the commercial ES powder (grey) show a sharp decrease from 240 to 360 ˚C, declining steadily afterwards. The NCS-85 material (blue) was very stable up to 1000 ˚C and retained 86% of its weight. The weight of PANI-6/NCS-85 gradually decreased and eventually remained at 74% of its original weight. The PANI-6/NCS-85 (orange) exhibits a behavior that is intermediate between ES and NCS-85. Specifically, no significant decrease in mass is observed between 240-360 C, unlike for the ES powder. Significantly more mass loss than for pure carbon was observed when the temperature reached 1000 ˚C (74 % vs 86% for PANI-6/NCS-85 vs. NCS 85, respectively). The drop in weight of the ES at 240 ˚C is due to the loss of dopants, followed by a steady weight loss afterwards, which is caused by PANI degradation. In the case of PANI-6/NCS-85, this degradation could lead to the formation of an N-

doped carbon material.[1–3] The NCS membrane is much more stable than ES because it was prepared by carbonization at 900 ˚C in N_2.

Another goal of the TGA analysis was to confirm the amount of PANI that was deposited inside the NCS. As seen from **Fig. S6,** the PANI-6/NCS-85 material retained 74% of its weight, giving a PANI content of 26 wt.%, assuming that it was completely burned. This value is fully consistent with the elemental analysis results (28 wt% PANI, **Table S2**). Note that parallel work showed identical behavior for the NCS-50/PANI composites and thus these results are not shown here.

Table S2. Elemental Analysis of PANI-6/NCS-85 Film

Element	Weight %
Carbon	86.3
Hydrogen	1.8
Nitrogen	4.2
PANI *	28

***** Elemental analysis of PANI-6/NCS-85 gives the content of nitrogen in the composite, which is 4.2 wt.% (Table S2). By assuming all of the nitrogen comes from polyaniline, the theoretical polyaniline content in PANI-6/NCS-85 is calculated to be 28 wt.%.

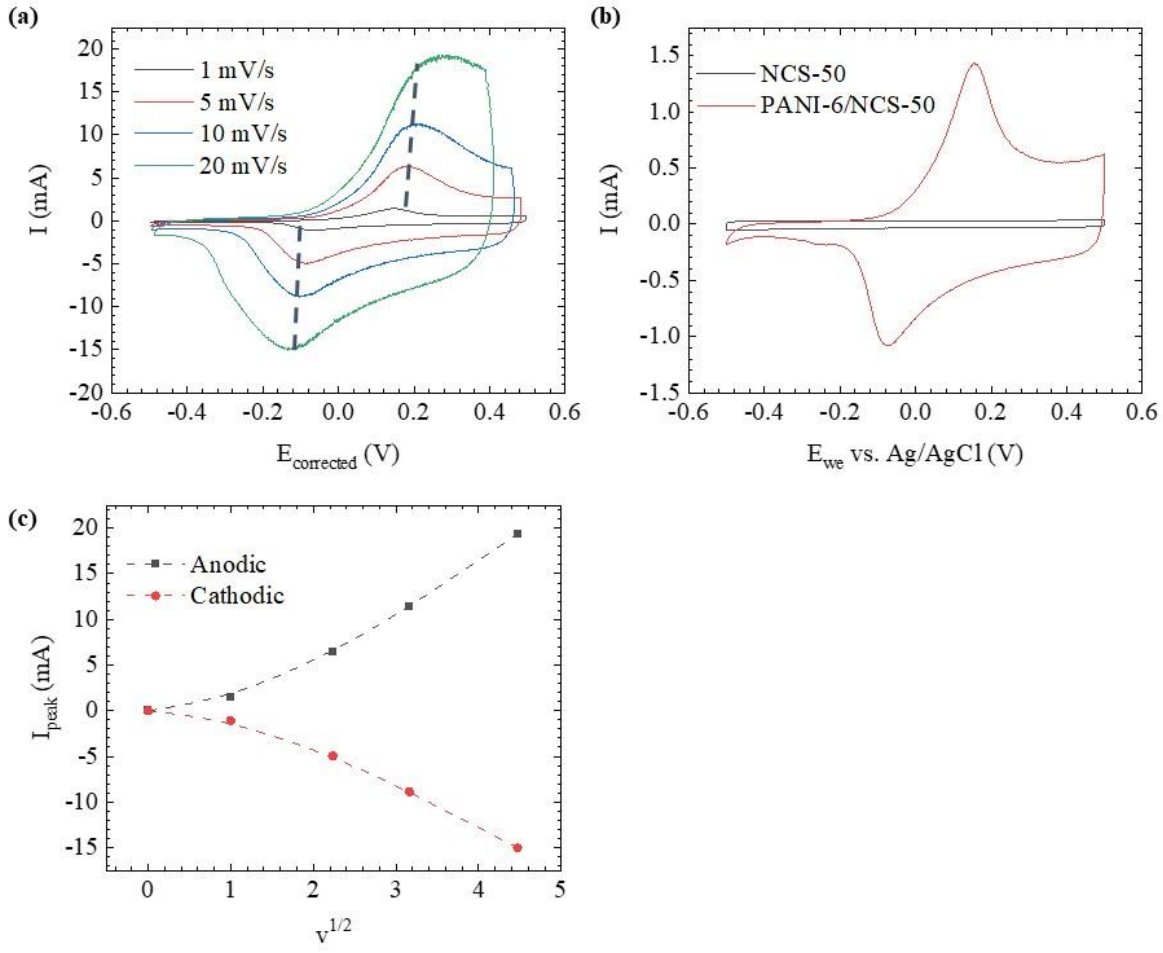

Figure S7. IR-corrected CVs of (a) PANI-6/NCS-50 at various sweep rates (1, 5, 10 and 20 mV/s) in 3 M NaCl, and (b) NCS-50 and PANI-6/NCS-50 at a scan rate of 1 mV/s in the same solution. (c) Relationship between the peak current (I_{peak}) and the square root of the sweep rate ($v^{1/2}$) of PANI-6/NCS-50.

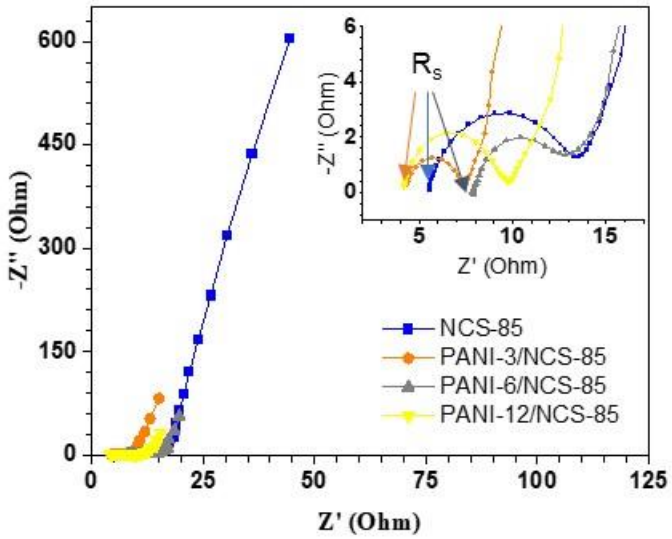

Figure S8. EIS response (plotted as Nyquist plots) of NCS-85 and PANI-X/NCS-85 composites, measured at the open circuit potential from 100 kHz to 10 mHz, with an ac amplitude of 10 mV, all in 3 M NaCl. The bulk electrolyte resistance (R_s) corresponds to the intercept of the plots with the real Z' axis at high frequencies (arrows).

References

(1) Vinu, A.; Anandan, S.; Anand, C.; Srinivasu, P.; Ariga, K.; Mori, T. Fabrication of Partially Graphitic Three-Dimensional Nitrogen-Doped Mesoporous Carbon Using Polyaniline Nanocomposite through Nanotemplating Method. *Microporous Mesoporous Mater.* 2008, *109* (1–3), 398–404. https://doi.org/10.1016/j.micromeso.2007.05.037.

(2) Han, J.; Xu, G.; Ding, B.; Pan, J.; Dou, H.; MacFarlane, D. R. Porous Nitrogen-Doped Hollow Carbon Spheres Derived from Polyaniline for High Performance Supercapacitors. *J. Mater. Chem. A* 2014, *2* (15), 5352–5357. https://doi.org/10.1039/c3ta15271e.

(3) Zhu, T.; Zhou, J.; Li, Z.; Li, S.; Si, W.; Zhuo, S. Hierarchical Porous and N-Doped Carbon Nanotubes Derived from Polyaniline for Electrode Materials in Supercapacitors. *J. Mater. Chem. A* 2014, *2* (31), 12545–12551. https://doi.org/10.1039/c4ta01465k.